AD

AMRA TR 66-36

AMRA TR 66-36

STRESS CONCENTRATION FACTORS IN T-HEADS

TECHNICAL REPORT

by

FRANCIS I. BARATTA

NOVEMBER 1966

Distribution of this document is unlimited

U. S. ARMY MATERIALS RESEARCH AGENCY
WATERTOWN, MASSACHUSETTS 02172

24

Mention of any trade names or manufacturers in this report shall not be construed as advertising nor as an official indorsement or approval of such products or companies by the United States Government.

The findings in this report are not to be construed as an official Department of the Army position, unless so designated by other authorized documents.

DISPOSITION INSTRUCTIONS

Destroy this report when it is no longer needed. Do not return it to the originator.

STRESS CONCENTRATION FACTORS IN T-HEADS

Technical Report AMRA TR 66-36

by

Francis I. Baratta

November 1966

D/A Project 1N542718D387

AMCMS Code 5547.12.62700

Projectile XM 474/573

Subtask 35425

Distribution of this document is unlimited.

U. S. ARMY MATERIALS RESEARCH AGENCY

WATERTOWN, MASSACHUSETTS 02172

U. S. ARMY MATERIALS RESEARCH AGENCY

STRESS CONCENTRATION FACTORS IN T-HEADS

ABSTRACT

Two simple formulae are presented which predict stress concentration factors applicable to a two-dimensional symmetrical T-head configuration. This configuration consists of a deep head joined to a shank by fillet radii. The independent equations that predict stress concentration factors for the same geometry are derived for two different loading conditions. In one instance, a tensile force is applied to the shank end of the T-shape. Equilibrium of forces is attained by supporting the bottom edge of the head section, resulting in the shank section being pulled in tension. In the second instance, a compressive load is applied to the top edge of the head section while the configuration is again supported at the bottom edge. Thus, only the head section is stressed and in a compressive manner.

Because the analysis is not exact, the magnitudes of the stress concentration factors resulting from the predictive equations appear to be overly conservative at some ranges of the geometry parameter ratios. Therefore, an arbitrary "limit of application", as it is termed in the text, is recommended when using these equations.

Again, because of the inexactness of the analysis, experimental stress concentration factors are indirectly obtained for the first loading condition and directly obtained for the second loading condition mentioned above. These data were obtained for several geometric ratios of the T-head configuration and compared to the corresponding predicted values.

It was found that the formulae could be utilized, with engineering accuracy, within a certain range of the two pertinent geometry ratios. Beyond these ranges, the error became excessive, but conservative.

CONTENTS

INTRODUCTION

A brief literature survey is presented of past work relating to stress concentration factors in two-dimensional T-head configurations. The results of the survey are pertinent to subsequent discussions. Hetenyi[1] was one of the first experimenters to test a two-dimensional T-head configuration. He stressed the body in a similar but slightly different manner than that shown in Figure 1a. The results were applicable for geometries which included several h/d ratios but only one d/R ratio. Twenty years later Hetenyi presented additional results[2] which were an extension of Reference 1. Heywood[3] further applied an empirical formula to the initial results of Hetenyi. His objective was to extrapolate Hetenyi's data by including the effect of d/R for T-heads of various h/d ratios. Nishihara and Fujii[4] obtained, by elasticity theory, the stress distribution in a two-dimensional bolt head. Although the results of this reference yield the desired stress concentration factor, the formulae are complicated and applicable over a limited range.

The objective of this report is to obtain an expression for the stress concentration factor associated with the configuration and loading shown in Figure 1a. The formula is developed because:

a. the empirical expression given in Reference 3 is based on the limited data of Reference 1; and

b. the formulae of Reference 4 are not amenable to simple computations and are inaccurate at some ratios of d/R of practical interest.

Formulae are obtained by superposition of various loading cases of Figure 1 which are guided by experimental observation. Two expressions, which yield values of the stress concentration factors applicable to Figures 1a and 1c, result from this analysis. These formulae increase the usable range of existing data and are easy to apply. However, because of the apparent conservativeness of the resulting equations at some ranges of the geometry parameters, a limit of application is suggested in the text. Also, since these formulae are not exact, experimental verification is provided.

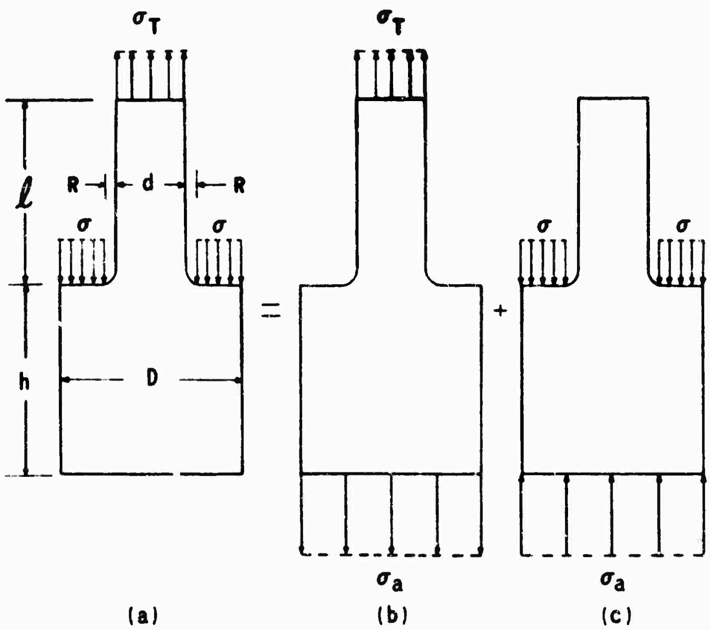

Figure 1. SUPERPOSED T-HEADS LOADINGS

FORMULATION

Photographs of models loaded similarly to those shown in Figures 1b and 1c are presented in Figures 2a and 2b. In particular, note the isochromatic fringe distribution at the fillets. An experimental determination of the location of these fringes at the fillet periphery for both loading cases revealed that for this model which had a large D/d ratio:

a. the stress gradient at and near the maximum stress site was relatively small; and

b. these regions for the two loading cases overlapped.

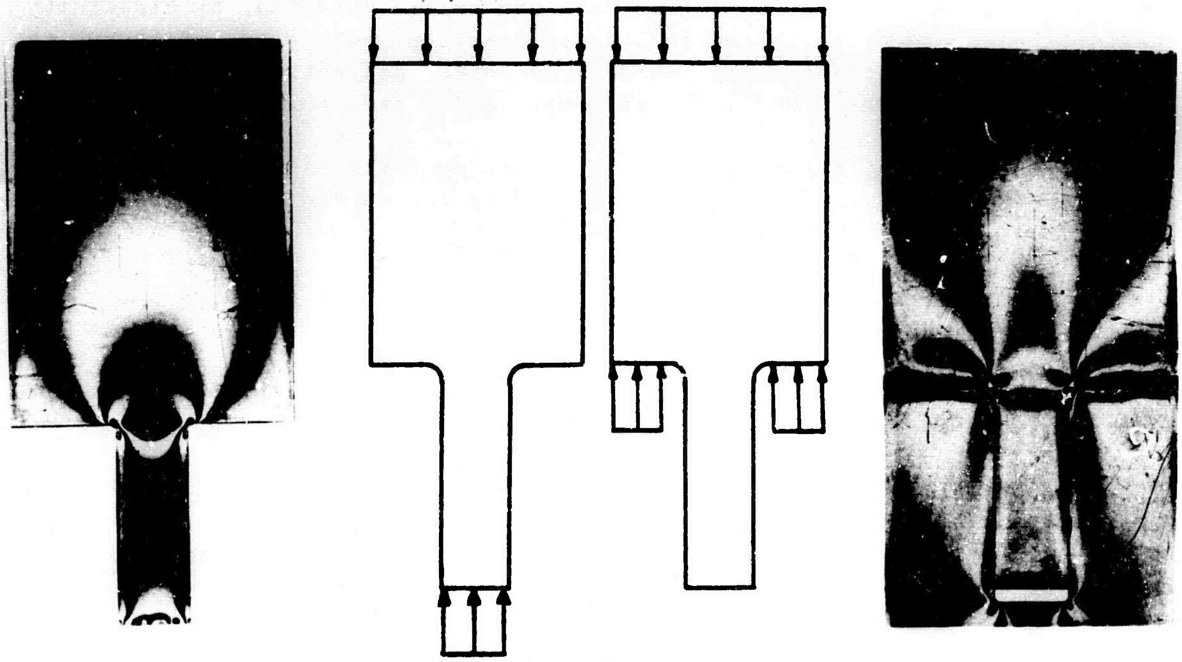

a. APPLIED LOAD 260 POUNDS **b. APPLIED LOAD 580 POUNDS**

Figure 2. ISOCHROMATIC PATTERN
Case IA, D/d = 4.0, d/R = 10.0

As the D/d ratio was reduced, while retaining a constant d/R ratio, the above statements became less correct. Even so, it shall be assumed hereafter that the maximum stress for the two loading cases occur at the same location and can be added or superimposed. The limitation on such an assumption will subsequently be determined. However, the maximum principal stresses at the fillets of Figures 1b and 1c are superimposed to obtain an approximate relationship for the maximum principal stresses at the fillets of Figure 1a. This relationship is given by the following formula:

$$\sigma_{fT} \simeq \sigma_{fa} + \sigma_{fc}, \qquad (1)$$

where σ_{fT}, σ_{fa}, and σ_{fc} are the maximum principal stresses at the fillets of Figures 1a, 1b, and 1c.

The stress concentration factors for the loading cases shown in Figure 1 are defined as follows:

$$k_{fT} = \frac{\sigma_{fT}}{\sigma_T}$$

$$k_{fa} = \frac{\sigma_{fa}}{\sigma_T} \tag{2}$$

and

$$k_{fc} = -\frac{\sigma_{fc}}{\sigma_a(D/d)},$$

where σ_T and σ_a are the uniformly applied stresses.

The sign convention adopted for the above stress concentration factors is as follows:

a. positive when the examined stress is the same sign (tension or compression) as the nominal stress to which it is compared; and

b. negative when the examined stress is the opposite sign to the nominal stress.

Substitution of Equations 2 into Equation 1 [note $\sigma_T = \sigma_a$ (D/d)] results in a relationship among the three stress concentration factors, given by the following:

$$k_{fT} \simeq k_{fa} - k_{fc}. \tag{3}$$

Thus, it is seen that the three concentrators associated with Figure 1 are directly superposable, if it can be assumed that maximum stresses are coincident.

It remains to obtain a relationship between the stress concentrators, k_{fa} and k_{fc}, to reduce the number of variables in Equation 3 to one. Accomplishment of this is realized by equating the loading state represented by Figure 1b, for which the stress concentration factor k_{fa} is experimentally well known,[5-10] to the sum of the two loading states shown in Figures 3b and 3c. Figure 3b can, in turn, be reduced to the same loading cases as those shown in Figures 1b and 1c, in which it is again assumed that the points of maximum stress of the two cases coincide. Therefore, the stress states represented by the loading cases shown in Figures 3b and 3c are superposable and result in the following formula:

$$\sigma_{fa} \simeq \sigma_{fb} + \sigma_{fc}, \tag{4}$$

where σ_{fb} is the maximum principal stress at the fillet of the configuration and loading shown in Figure 3b.

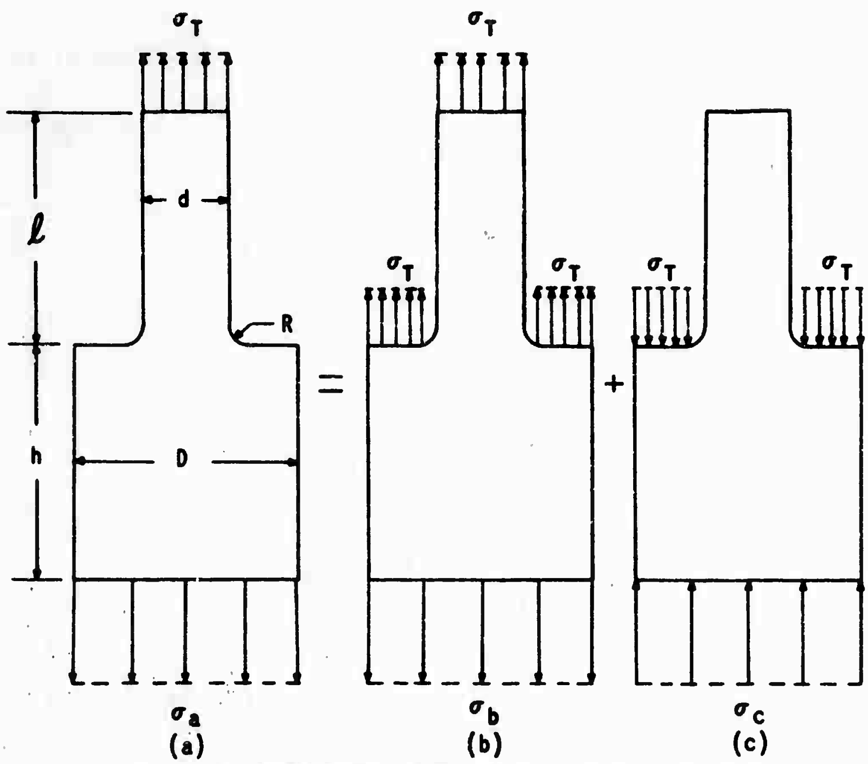

Figure 3. SUPERPOSED LOADINGS OF T-HEAD IN TENSION

It was indicated in Reference 11 that if the stress loading σ_T could have been applied to all horizontal surfaces of the configuration shown in Figure 3b as well as on the fillet radii, then the stress concentrator would be exactly equal to one. It was considered impracticable to accomplish this loading exactly by experimental means. However, it was found that as long as the fillet radius was small relative to the neck width d the stress at the fillet σ_{fb} tended to be equal to the applied stress σ_T when the stress loading and configuration were the same as that shown in Figure 3b. Thus, Equation 4 can be reduced to the following:

$$\sigma_{fa} \simeq \sigma_T + \sigma_{fc} \quad \text{(R/d be small)}. \tag{5}$$

Defining the stress concentration factors k_{fa} and k_{fc} in terms of the applied stress shown in Figures 3a and 3c, we have:

$$k_{fa} = \frac{\sigma_{fa}}{\sigma_T}$$

and

$$k_{fc} = - \frac{\sigma_{fc}}{\sigma_c (D/d)}.$$

Substitution of the above into Equation 5 and consideration of the equilibrium of forces on the body shown in Figure 3c yields:

$$k_{fa} + (D/d - \frac{2}{d/R} - 1)\, \kappa_{fc} = 1 \tag{6}$$

or

$$k_{fc} \approx - \frac{k_{fa} - 1}{D/d - \frac{2}{d/R} - 1} . \quad (7)$$

(For physically significant geometry D-d-2R>0 and D/d-1-2/d/R>0).

Substitution of Equation 7 into Equation 3 for k_{fT} finally results in the following formula:

$$k_{fT} \approx \frac{k_{fa} (D/d - \frac{2}{d/R}) - 1}{D/d - \frac{2}{d/R} - 1} . \quad (8)$$

As previously indicated, experimental data are available for the stress concentration factor k_{fa} for various D/d and d/R ratios. However, an empirical formula is given by Heywood in Reference 3 for this concentrator based on the experimental data available. Heywood's equation becomes (using the nomenclature in this report):

$$k_{fa} \approx 1 + \left[\frac{(D/d - 1)\ d/R}{2(2.8\ D/d - 2)}\right]^{0.65} . \quad (9)$$

This empirical relationship can be utilized to obtain formulae for the stress concentrators k_{fT} and k_{fc}, which are dependent upon only the geometry ratios D/d and d/R. Direct substitution of Equation 9 into Equations 7 and 8 results in the following relationships:

$$k_{fT} \approx \frac{\left\{1 + \left[\frac{(D/d - 1)\ d/R}{2(2.8\ D/d - 2)}\right]^{0.65}\right\} (D/d - \frac{2}{d/R}) - 1}{D/d - \frac{2}{d/R} - 1} \quad (10)$$

and

$$k_{fc} \approx - \frac{\left[\frac{(D/d - 1)\ d/R}{2(2.8\ D/d - 2)}\right]^{0.65}}{D/d - \frac{2}{d/R} - 1} . \quad (11)$$

The reader is cautioned that Equations 8 and 10 are invalid for small values of h/d (see Figure 1) since bending of the flanges of the head is precluded from the analysis. Hetenyi[2] indicates that when h/d is equal to 3.0 or greater, the head of the T can be considered infinitely deep, thus eliminating the existence of bending stresses at the fillet.

A more useful definition of the stress concentration factor for the configuration shown in Figure 3c is $k'_{fc} = - \sigma_{fc}/\sigma_c$, and from Equation 2 we see that $k'_{fc} = k_{fc}$ D/d. Substitution of this latter relationship into Equation 11 results in the following:

$$k'_{fc} \approx - \frac{D/d \left[\frac{(D/d - 1)\ d/R}{2(2.8\ D/d - 2)} \right]^{0.65}}{D/d - \frac{2}{d/R} - 1} . \qquad (12)$$

LIMIT OF APPLICATION

The stress concentration factors, k_{fT} and k'_{fc}, described by Equations 10 and 12, are shown plotted as a function of the constant parameter D/d and variable d/R in Figures 4a and 4b. There are distinct minimum values for each curve described by D/d in these figures. As previously indicated, it would seem that as d/R is decreased, k_{fT} and k'_{fc} should also decrease (which they do up to a point) and asymptotically approach a minimum value (which they do not). It is evident that this behavior is not correct and occurs as a result of inexactness of the equations which in turn could be caused by:

a. the approximate nature of the observation that the maximum principal stresses occur at the same fillet locations; and

b. the violation of the restriction that the radius R be small compared to the width d.

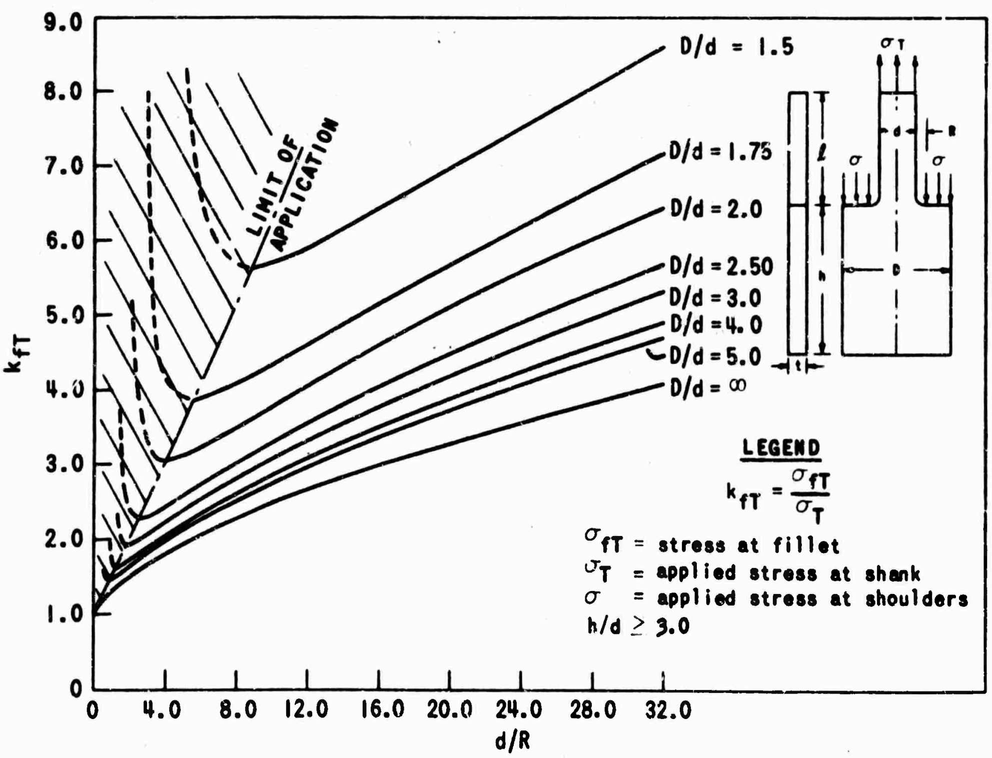

Figure 4a. STRESS CONCENTRATION FACTOR k_{fT}

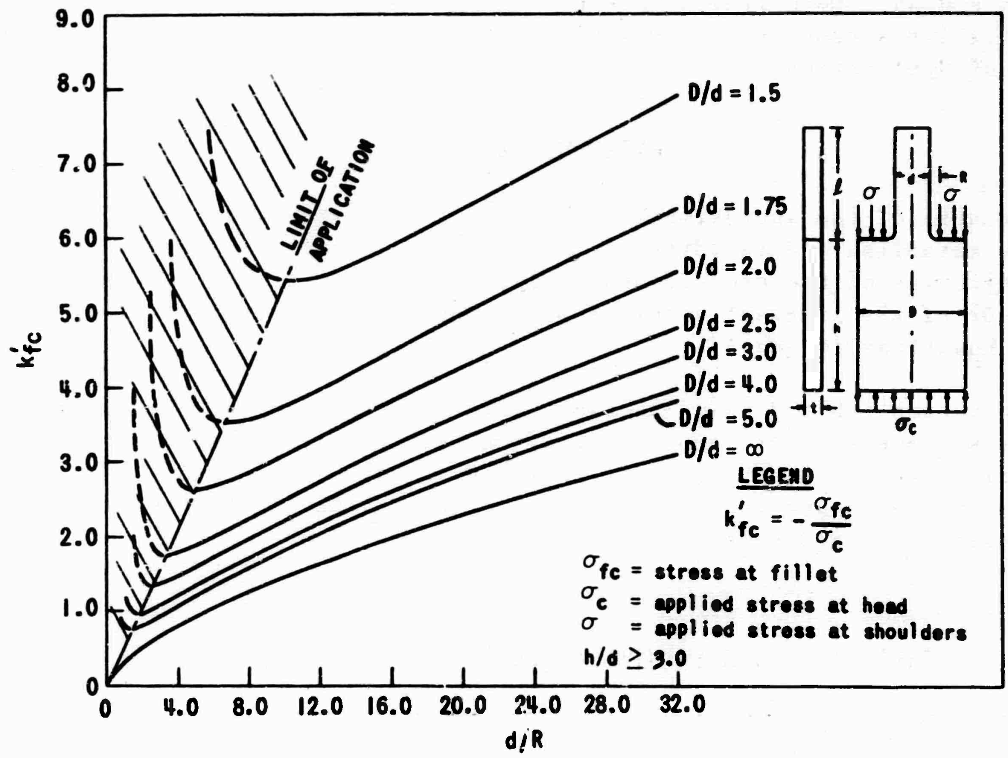

Figure 4b. STRESS CONCENTRATION FACTOR k'_{fc}

Thus, the accuracy and application of the expressions beyond the minimum points are questionable. The seemingly odd behavior indicated above will provide convenient practical cut-off points for each curve describing k_{fT} and k'_{fc}. (The cut-off points are experimentally checked for two cases and are discussed later). These cut-off points can be determined by the minimum values of the stress concentration factors defined by particular values of d/R as a function of D/d. These minimum values will provide limits on the use of Equations 10 and 12 and shall be called "limits of application".

The limits are analytically determined by simply applying maximum-minimum principles to Equations 10 and 12. The limits of application of Equation 10 describing k_{fT} are given in the following:

$$d/R \geq \frac{2}{D/d - 1/2\,(1-1/n) - \sqrt{(1/n)(D/d) + 1/4\,(1-1/n)^2}} \,. \tag{13}$$

The limits of application of Equation 12 describing k'_{fc} are given by

$$d/R \geq \frac{2(1+n)}{n(D/d-1)} \tag{14}$$

where n = 0.65. Both limits have been computed and are shown in Figures 4a and 4b as lines connecting the minimum point in each curve and are labeled "limit of application".

EXPERIMENTAL STUDY

Because of the approximations used in the previous section it was necessary to establish the validity of the derived equations. Therefore, the primary objective of the experimental program was to determine the order of magnitude of the inherent error associated with the determination of k_{fT} and k'_{fc} by Equations 10 and 12.

To accomplish the above in the simplest manner, the stress concentration factors k_{fa} and k'_{fc} were experimentally determined for four cases which had the various geometry ratios shown in Table I. The stress concentration factor k_{fT} was then obtained from these data for each of the four cases by simple superposition as indicated by Equation 3.

Table I. EXPERIMENTAL, SUPERPOSED, AND PREDICTED DATA

			EXPERIMENTAL DATA			SUPERPOSED DATA		PREDICTED DATA			
							Combined Factor, Equation 6				
Case	d/R	D/d	k_{fa}	k'_{fc}	k_{fc}	k_{fT}*	$k_{fa} + (D/d - \frac{2}{d/R} - 1)k_{fc} = 1.0$	k_{fT}†	Percent difference	k'_{fc}‡	Percent difference
IA	10.0	4.0	2.37	-2.05	-0.51	2.88	0.94	2.86	- 0.7	-1.96	- 4.4
IB	10.0	2.0	2.25	-2.48	-1.24	3.49	1.27	3.79	+ 8.6	-3.10	-25.0
IC**	10.0	1.5	1.95	-2.71	-1.81	3.76	1.41	5.71	+51.8	-5.43	+ 100
II**	5.1	2.0	1.95	-1.08	-0.54	2.49	1.62	3.13	+25.7	-2.65	+ 145

*Obtained by superposing k_{fa} and k_{fc} according to Equation 3.

†Computed according to Equation 10.

‡Computed according to Equation 12.

**Limit of application case for k'_{fc}.

NOTE: $\frac{h}{d} \geq 3.0$

Cases IC and II were designed to determine the maximum error allowed by the limit of application. The geometries for these cases were determined according to the limit of application on the concentrator k'_{fc}, (Equation 14) rather than k_{fT}. This was done because the minimum points for k'_{fc} as shown in Figure 4b are slightly more limiting than the corresponding curves in Figure 4a. Thus, for the same D/d value the limiting d/R ratio is greater for k'_{fc} than for k_{fT}, and, therefore, more restricted.

The experimental data were obtained by a photoelastic study using a model made of Homalite 100. The two methods of applying the load and the model dimensions for the four cases investigated are shown in Figure 5. The model was compressively stressed* by the first method of loading, Figure 5a, then by the second method, Figure 5b. The photoelastic model was stressed by the first method to determine the factor k_{fa}, the location of the maximum fringe order, and to index this maximum stress site by scribing fiduciary lines on the model. At this location the fringe order was also determined when the model was loaded by the second method. Thus, the nominal fringe order at the shank section N_d, the maximum fringe order at the fillet N_{fa}, and at this same site the fringe order N_{fc}, were obtained for each case and are shown plotted as functions of load in Figures 6 and 7. These experimental data were then utilized to obtain the stress concentration factors k_{fa} and k_{fc}, from which k_{fT} was indirectly determined.

Figures 2a and 2b are photographs of the isochromatic fringe patterns, with a light background resulting from the two loading methods chosen as representative of typical patterns of case IA (d/D = 4.0 and d/R = 10.0).

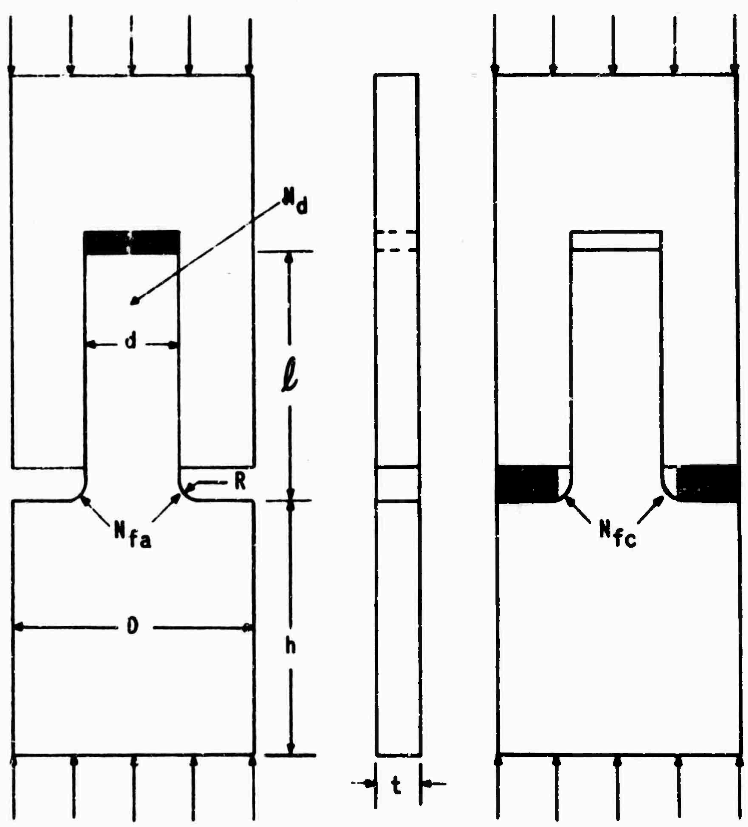

(a) (b)

	CASE			
	IA	IB	IC	II
R	0.075	0.075	0.075	0.110
d	0.750	0.750	0.750	0.565
D	3.000	1.500	1.125	1.125
ℓ	2"	2"	2"	2"
h	7"	5"	5"	5"
t	1/2"	1/2"	1/2"	1/2"

NOTES:

1. DECIMAL TOLERANCE IS ± 0.001"
2. SHADED AREAS SHOW CARDBOARD PAD LOCATIONS

Figure 5. LOADING AND MODEL PARAMETERS

*Pads were used at all contact surfaces to simulate a constantly distributed load.

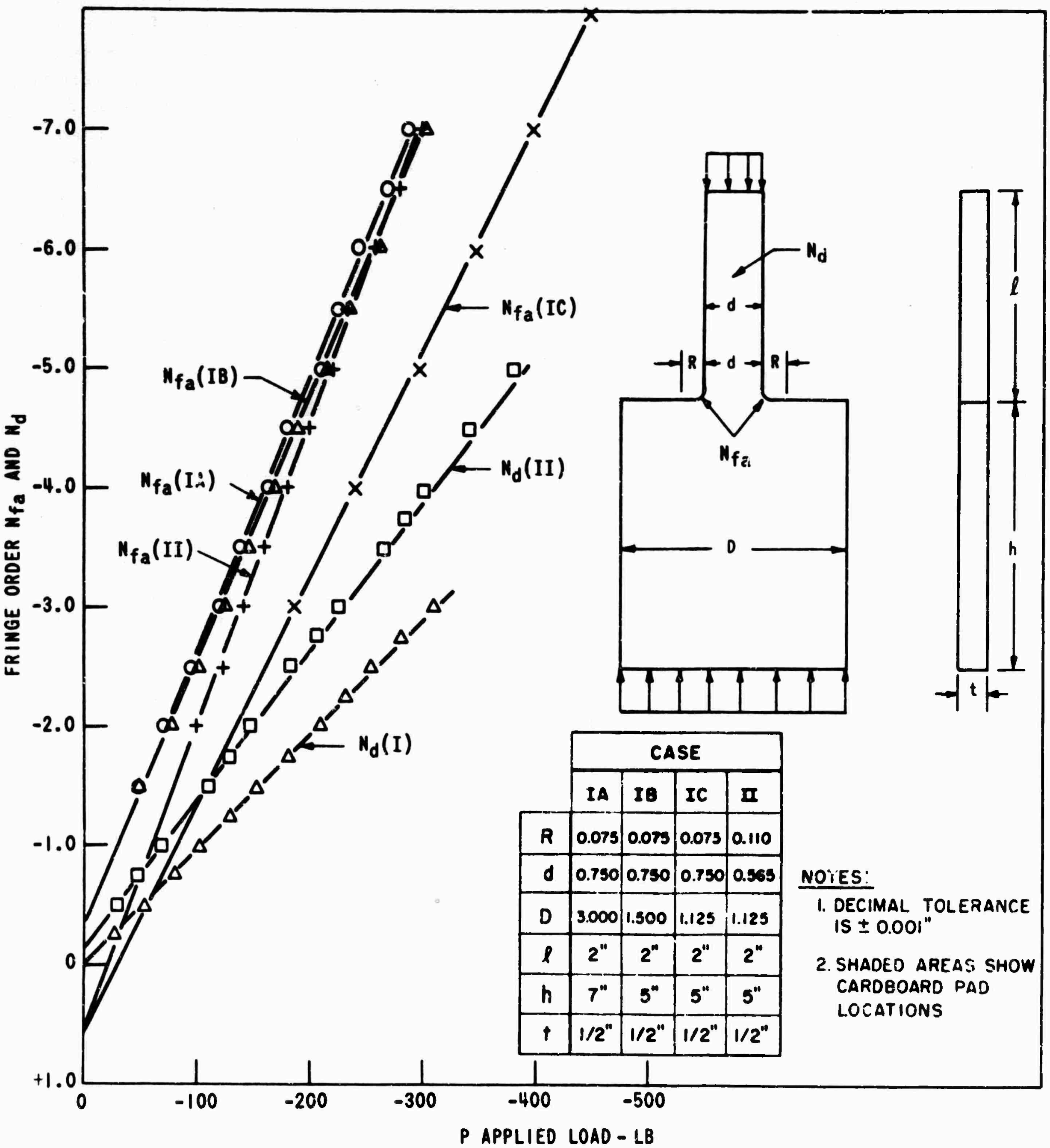

	CASE			
	IA	IB	IC	II
R	0.075	0.075	0.075	0.110
d	0.750	0.750	0.750	0.565
D	3.000	1.500	1.125	1.125
ℓ	2"	2"	2"	2"
h	7"	5"	5"	5"
t	1/2"	1/2"	1/2"	1/2"

NOTES:

1. DECIMAL TOLERANCE IS ± 0.001"
2. SHADED AREAS SHOW CARDBOARD PAD LOCATIONS

Figure 6. FRINGE ORDER N_{fa} AND N_d AS A FUNCTION OF APPLIED LOAD

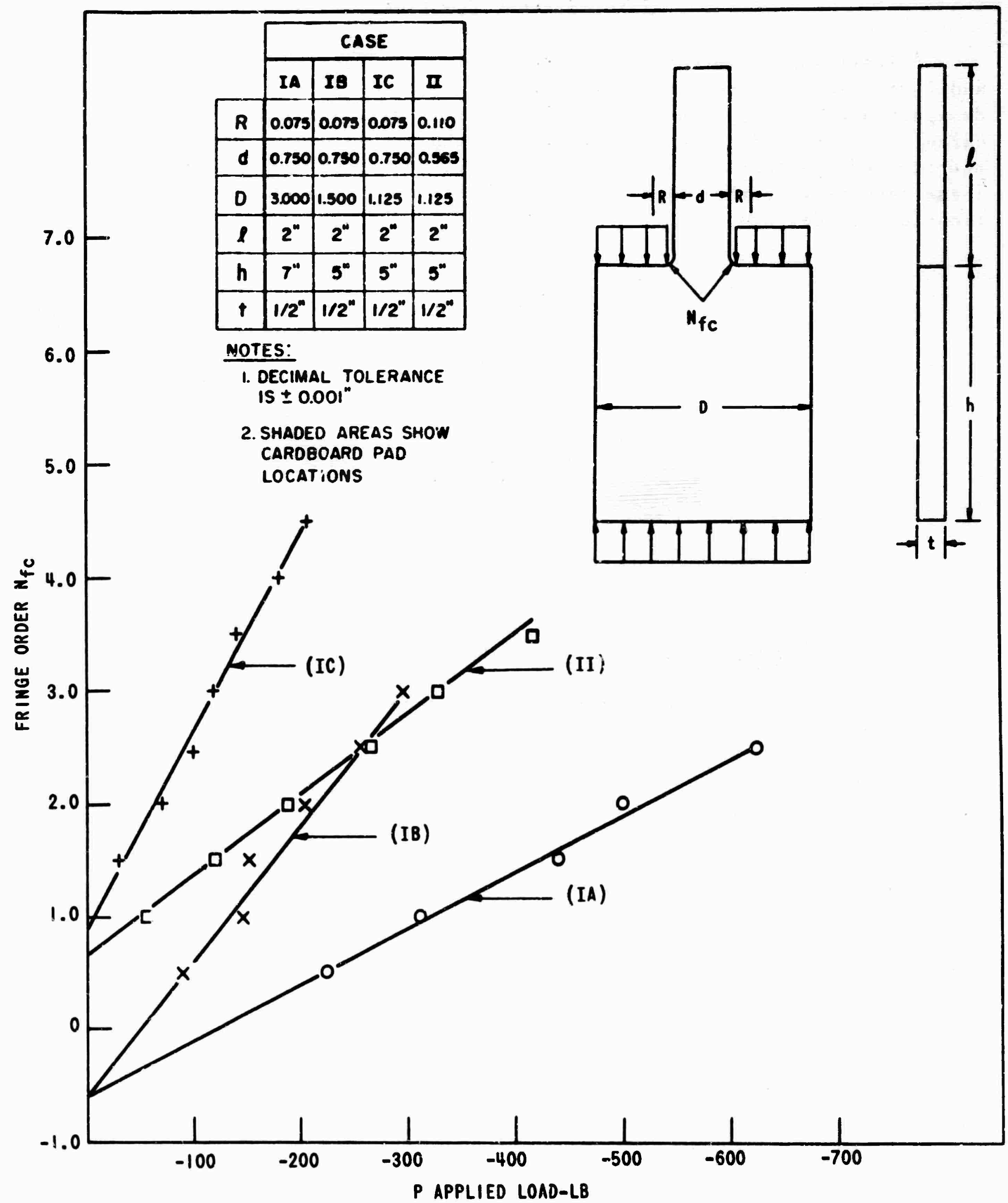

Figure 7. FRINGE ORDER N_{fc} AS A FUNCTION OF APPLIED LOAD

RESULTS AND DISCUSSION

A least-square method which incorporated the data shown in Figures 6 and 7 was used to determine accurately the equation of each straight line designated by N_d, N_{fa}, and N_{fc} for all cases. A straight-line fit for each curve was corrected to initiate at the origin of the plot. Residual stresses and time edge effects present in the photoelastic model were thus compensated. These results were then used to determine the desired experimental concentration factors defined as:

$$k_{fa} = \frac{N_{fa}}{N_d}$$

$$k_{fc} = \frac{N_{fc}}{N_d}$$

$$k_{fT} = \frac{N_{fa} - N_{fc}}{N_d}$$

and

$$k'_{fc} = k_{fc}(D/d).$$

The stress concentration factors for each case are shown in Table I.

It is noted that in the formulation of Equation 6, it was necessary to make use of:

a. an experimental approximation, i.e., it was assumed that the points of maximum stress of the loading cases shown in Figures 1b and 1c coincided;

b. an experimental fact, i.e., from Reference 10 it was determined that under idealized conditions the stress concentrator would be equal to 1.0; and

c. the restriction that the fillet radius R be small compared to the small width d.

If all of the above were true, the left side of Equation 6, which is termed the Combined Factor, would be equal to unity (1.0). This Combined Factor could be used as an index, when compared to 1.0, on the relative accuracy of Equations 10 and 12, which predict k_{fT} and k'_{fc}. The Combined Factor, for which the computations were based on the experimentally determined concentrators k_{fa} and k_{fc}, as well as the predicted values of k_{fT} and k'_{fc}, and the percent difference when compared to experimental values are also given in Table I.

Results given in Table I indicate that when d/R is constant (see cases IA, IB, and IC), the Combined Factor approaches the idealized value of 1.0 with increasing D/d. Also, when D/d is constant but d/R is increased, as in cases II and IB, the Combined Factor appears to approach the idealized value of 1.0. It is apparent from Table I that as the Combined Factor approaches 1.0, the percent differences for both k_{fT} and k'_{fc} become small. These differences are based on a comparison of experimental values of k_{fT} (and superposed data) and k'_{fc} to those given by the predictive equations 10 and 12. Further examination of these relative differences reveals that:

1. k_{fT} determined by Equation 10 is accurate, compared to the experimental value (see superposed data), to within less than 9.0% if $D/d \geq 2.0$ and $d/R \geq 10.0$ (compare cases IA and IB to case IC).

2. k'_{fc} determined by Equation 12 is accurate to within 25.0% if $D/d \geq 2.0$ and $d/R \geq 10.0$ when related to the experimental data (compare cases IA and IB to case IC).

3. The two cases, IC and II, which are at the limit of application for the concentrator k'_{fc}, yield the maximum differences, 100% and 145%, respectively. However, these differences are positive and are considered conservative.

Comparisons can also be made to the data given in References 1 and 2 by Hetenyi even though the loading configuration used by this author, shown in Figure 8a, is different from that shown in Figure 8b. The difference between these two loading states is shown in Figure 8c. It is readily apparent that if the fillet radius R is small, the Hetenyi-type stress concentration factor termed here as k_{fH} is approximately equivalent to k_{fT}. The data from References 1 and 2 are presented in Table II as well as the predicted values of the stress concentration factor k_{fT} given by Equation 10, and the percent error when compared to k_{fH}.

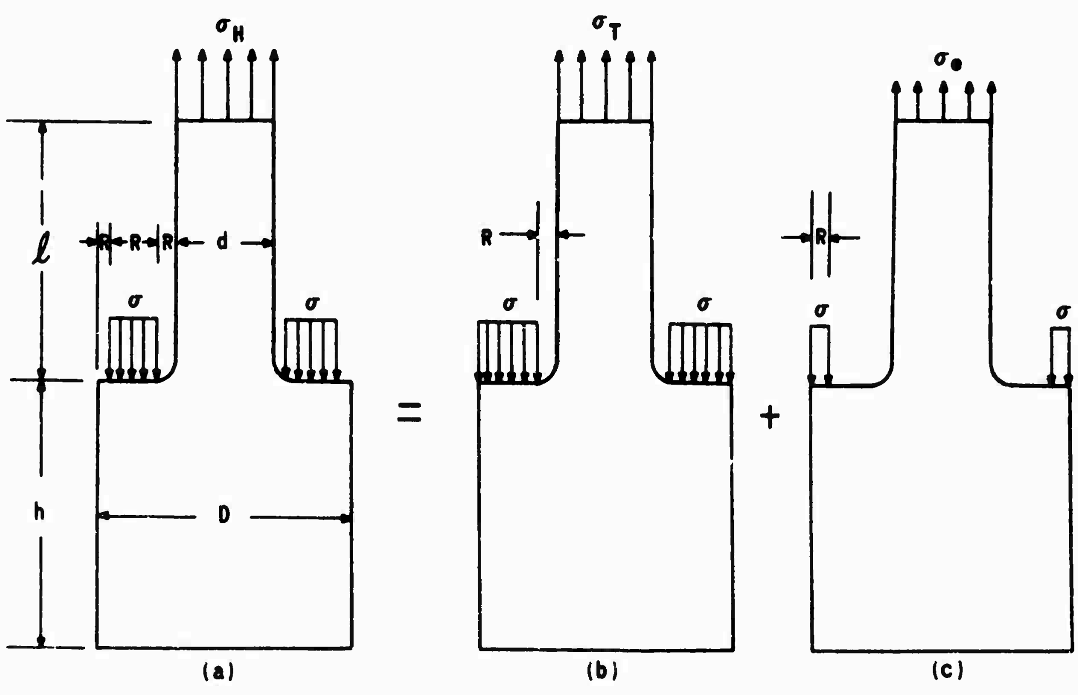

Figure 8. HETENYI TYPE T-HEADS

Table II. COMPARISON TO EXPERIMENTAL RESULTS OF T-HEADS AVAILABLE IN THE LITERATURE

Hetenyi's Results - References 1 and 2

D/d	d/R = 20.0			d/R = 13.33			d/R = 10.0			d/R = 5.0		
	k_{fH}	k_{fT}*	% error	k_{fH}	k_{fT}*	% error	k_{fH}	k_{fT}*	% error	k_{fH}	k_{fT}*	% error
3.0	4.10	4.20	+ 2.4	3.50	3.48	- 0.6	3.10	3.08	- 1.0	2.52	2.38	- 5.6
2.5	4.47	4.50	- 1.0	3.65	3.73	+ 2.2	3.02	3.30	+ 9.3	2.35	2.58	+ 9.8
2.0	5.00	5.10	+ 2.0	3.90	4.25	+ 9.0	3.30	3.79	+14.8	2.60	3.10	+19.2
1.5	6.05	6.97	+15.0	4.90	6.05	+24.0	4.70	5.71	+21.5	-	-	-

*Computed according to Equation 10 (All values of k_{fT} are within the limit of application given by Equation 13)

NOTE: $\frac{h}{d} \geq 3.0$

A comparison of the results given in Table II indicates that as D/d increases, with d/R remaining constant, the error generally decreases. This is because the points of maximum stress for the various loading cases tend to coincide and the stress gradient becomes small as D/d becomes large. The results also indicate that, generally, Equation 10 becomes more accurate as d/R increases, with D/d remaining constant. This is due to:

a. the restriction that the fillet radius R be small compared to the width d in the analysis; and

b. as R becomes small the Hetenyi-type concentration becomes equivalent to k_{fT}.

It is also seen from Table II that as the error becomes large, it is positive. Further, if one is interested in accuracy of 10% or better, then Equation 10 can be used when:

a. D/d is equal to or greater than 2.5 and d/R lies between 5.0 and 20.0; and

b. D/d is equal to or greater than 2.0 and d/R lies between 13.33 and 20.0.

Analytically computed results for the stress concentration factor k_{fT} as a function of d/R when D/d = 2.325 are given in Reference 4. These data, as well as those obtained from Equation 10, can readily be compared and are shown in Figure 9. It is seen that these curves compare to within at least 10% of each other when d/R is between 3 and 28; beyond the value of 28, the difference is excessive. As d/R increases, k_{fT} becomes more accurate. On the other hand, the mapping function utilized in Reference 4 becomes inexact for large values of d/R. This difference is attributed to the method used in Reference 4 when d/R > 28. However, it is expected that when d/R is small, the method given by Reference 4 is quite accurate.

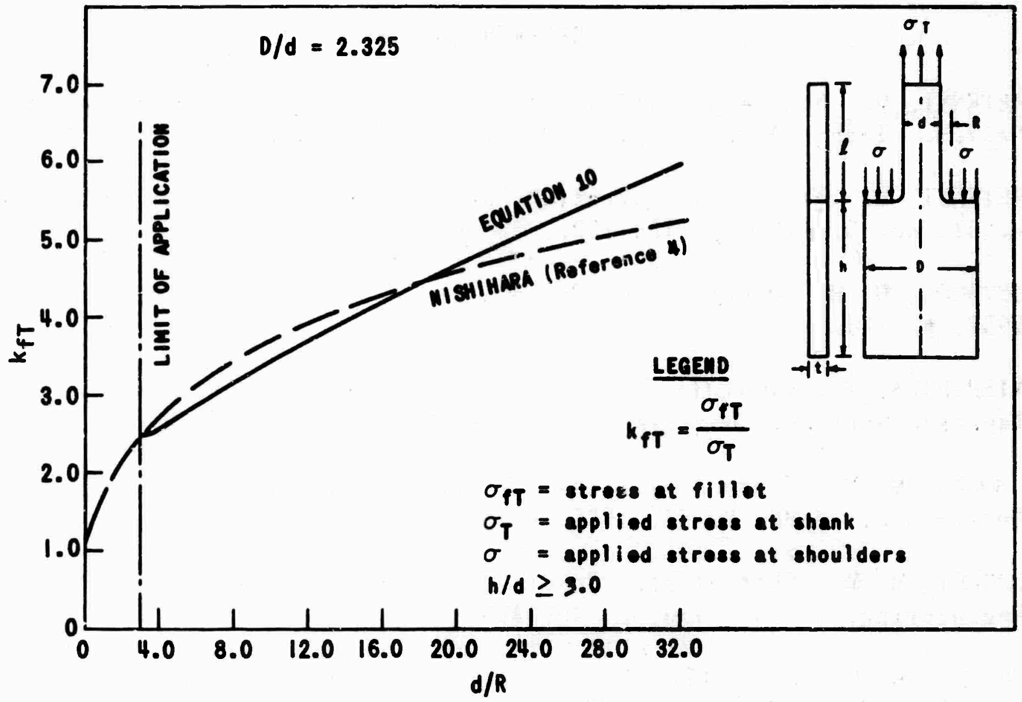

Figure 9. COMPARISON OF STRESS CONCENTRATION FACTOR k_{fT}

SUMMARY OF CONCLUSIONS

1. The difference between the experimentally determined concentrators, k_{fT} and k'_{fc}, and the equations used to predict them become quite small when either: (a) the ratio of d/R is increased, while retaining D/d as a constant parameter; or (b) the ratio of D/d is increased while retaining d/R as a constant parameter.

2. When compared to the experimental value, if $D/d \geq 2.0$ and $d/R \geq 10.0$, k_{fT} can be determined by Equation 10 within a difference of 9% or less. Equation 10 can be used in other ranges with a corresponding increase in the difference, which appears to be conservative. Alternatively, the formula of Reference 4 can be used in those regions.

3. The prediction of k'_{fc} by Equation 12 could be useful as a first-order approximation, and it is considered probable that the error in predicting this concentrator will be conservative.

4. The Hetenyi-type concentrator k_{fH} can be determined by Equation 10 within an error of 10% or less if: (a) $D/d \geq 2.5$ with d/R between 5.0 and 20.0; and (b) $D/d \geq 2.0$ with d/R between 13.33 and 20.0.

ACKNOWLEDGMENT

The author gratefully acknowledges the constructive criticisms and suggestions given by Mr. J. Adachi, which materially aided in realizing the final copy.

REFERENCES

1. HETENYI, M. *Some Applications of Photoelasticity in Turbine-Generator Design*. Trans. ASME, v. 61, 1939, p. A-151 to A-155.

2. HETENYI, M. *Stress-Concentration Factors for T-Heads*. J. Appl. Mech., v. 81, no. 3, 1959, p. 130-132.

3. HEYWOOD, R. B. *Designing by Photoelasticity*. Chapman & Hall Ltd., 1952, p. 178.

4. NISHIHARA, T., and FUJII, T. *Stresses in Bolt Head*. Proc. of First Japanese National Congress for Applied Mechanics, 1951, p. 145-150.

5. FROCHT, M. M. *Factors of Stress Concentration Photoelastically Determined*. ASME, V. 57, 1935, p. A-67.

6. FROCHT, M. M. *Photoelastic Studies in Stress Concentration*. Mechanical Engineering, v. 58, 1936, p. 485-489.

7. FROCHT, M. M., and LANDSBERG, D. *Factors of Stress Concentration in Bars with Deep Sharp Grooves and Fillets in Tension*. Proc. SESA, v. VIII, no. 2, 1951, p. 148.

8. TIMOSHENKO, S., and DIETZ, W. *Stress Concentration Produced by Holes and Fillets*. Trans. ASME, v. 47, 1925, p. 199-237.

9. WEIBEL, E. E. *Studies in Photoelastic Stress Determination*. Trans. ASME, v. 56, 1934, p. 637-658.

10. PETERSON, R. E. *Stress Concentration Design Factors*. John Wiley & Sons, 1953.

11. BARATTA, F. I., and BLUHM, J. I. *On the Nullification of Stress Concentration Factors by Stress Equalization*. U. S. Army Materials Research Agency, AMRA TR 66-37, November 1966. Presented at the June 1966 meeting of S.E.S.A. in Detroit.

U. S. ARMY MATERIALS RESEARCH AGENCY
WATERTOWN, MASSACHUSETTS 02172

TECHNICAL REPORT DISTRIBUTION

Report No.: AMRA TR 66-36 November 1966 Title: Stress Concentration Factors in T-Heads

---

Distribution List approved by Picatinny Arsenal, telephone conversation, 28 November 1966.

No. of Copies	To
1	Office of the Director, Defense Research and Engineering, The Pentagon, Washington, D. C. 20301
20	Commander, Defense Documentation Center, Cameron Station, Building 5, 5010 Duke Street, Alexandria, Virginia 22314
2	Defense Metals Information Center, Battelle Memorial Institute, Columbus, Ohio 43201
	Chief of Research and Development, Department of the Army, Washington, D. C. 20310
2	ATTN: Physical and Engineering Sciences Division
1	Commanding Officer, Army Research Office (Durham), Box CM, Duke Station, Durham, North Carolina 27706
	Commanding General, U. S. Army Materiel Command, Washington, D. C. 20315
1	ATTN: AMCPP, Mr. S. Lorber
1	AMCRD
1	AMCRD-RS
	Commanding General, U. S. Army Missile Command, Redstone Arsenal, Alabama 35809
5	ATTN: AMSMI-RBLD, Redstone Scientific Information Center
1	AMSMI-RRS, Mr. R. E. Ely
1	AMSMI-RKX, Mr. R. Fink
1	AMSMI, Mr. W. K. Thomas
1	AMSMI-RSM, Mr. E. J. Wheelahan
2	Commanding General, U. S. Army Mobility Command, Warren, Michigan 48090
	Commanding General, U. S. Army Munitions Command, Dover, New Jersey 07801
2	ATTN: Feltman Research Laboratories

No. of Copies	To
	Commanding General, U. S. Army Natick Laboratories, Natick, Massachusetts 01762
1	ATTN: Dr. J. Flanagan
	Commanding General, U. S. Army Tank-Automotive Center, Warren, Michigan 48090
2	ATTN: AMSMO-REM.1
	Commanding General, U. S. Army Test and Evaluation Command, Aberdeen Proving Ground, Maryland 21005
2	ATTN: AMSTE
	Commanding General, U. S. Army Weapons Command, Rock Island, Illinois 61202
1	ATTN: AMSWE-PP, Procurement and Production Directorate
1	AMSWE-TX, Research Division
1	AMSWE-IM, Industrial Mobilization Branch
	Commanding Officer, Harry Diamond Laboratories, Washington, D. C. 20438
1	ATTN: AMXDO, Library
	Commanding Officer, Frankford Arsenal, Philadelphia, Pennsylvania 19137
2	ATTN: Pitman-Dunn Institute of Research
	Commanding Officer, Picatinny Arsenal, Dover, New Jersey 07801
1	ATTN: SMUPA-TW, Nuclear Engineering Directorate
	Commanding Officer, Springfield Armory, Springfield, Massachusetts 01101
1	ATTN: SWESP-EG, Engineering Division
1	SWESP-TX, Research and Development Division
2	Commanding Officer, U. S. Army Mobility Command, Washington Liaison Office, Room 1719, Building T-7, Gravelly Point, Washington, D. C. 20315
	Commanding Officer, Watervliet Arsenal, Watervliet, New York 12189
1	ATTN: Mr. F. Dashnaw
	Chief, Bureau of Naval Weapons, Department of the Navy, Room 2225, Munitions Building, Washington, 20390
1	ATTN: RMMP
	Chief, Bureau of Ships, Department of the Navy, Washington, D. C. 20360
1	ATTN: Code 341
1	Chief, Naval Engineering Experimental Station, Department of the Navy, Annapolis, Maryland

No. of Copies	To
	Commander, Naval Ordnance Laboratory, White Oak, Silver Spring, Maryland 20910
2	ATTN: Code WM
	Commander, Naval Ordnance Test Station, China Lake, California 93555
1	ATTN: Code 5557
	Director, Naval Research Laboratory, Anacostia Station, Washington, D. C. 20390
1	ATTN: Technical Information Officer
	Commander, Naval Weapons Laboratory, Dahlgren, Virginia 22448
1	ATTN: A&P Laboratory
	Chief, Office of Naval Research, Department of the Navy, Washington, D. C. 20390
1	ATTN: Code 423
	Commander, Wright Air Development Division, Wright-Patterson Air Force Base, Ohio 45433
1	ATTN: WWRCO
1	AFRCWE-1
1	U. S. Atomic Energy Commission, Army Reactor Branch, Division of Research Development, Washington, D. C.
	U. S. Atomic Energy Commission, Division of Nuclear Materials Management, Washington, D. C.
1	ATTN: Mr. Alton F. Elder
	U. S. Atomic Energy Commission, Albuquerque Field Office, P. O. Box 4500, Albuquerque, New Mexico 87106
1	ATTN: Mr. N. MacKay, Nuclear Materials Management Office
1	U. S. Atomic Energy Commission, Office of Technical Information Extension, P. O. Box 62, Oak Ridge, Tennessee
1	U. S. Atomic Energy Commission, San Francisco Operations Office, 2111 Bancroft Way, Berkeley, California 94704
	National Aeronautics and Space Administration, 1520 H Street, N. W., Washington, D. C. 20546
1	ATTN: Mr. B. G. Achhammer
1	Mr. G. C. Deutsch
1	Mr. R. V. Rhode

No. of Copies	To
	National Aeronautics and Space Administration, Marshall Space Flight Center, Huntsville, Alabama 35812
1	ATTN: R-P&VE-M, Dr. W. R. Lucas
1	M-F&AE-M, Mr. W. A. Wilson
	Director, Jet Propulsion Laboratory, California Institute of Technology, 4800 Oak Grove Drive, Pasadena, California 91003
1	ATTN: Mr. Howard E. Martens, Materials Section 351
	Commanding Officer, U. S. Army Materials Research Agency, Watertown, Massachusetts 02172
5	ATTN: AMXMR-AT
1	AMXMR-AA
1	AMXMR-RP
1	AMXMR-RX
1	Author
90	TOTAL COPIES DISTRIBUTED

UNCLASSIFIED
Security Classification

DOCUMENT CONTROL DATA - R&D

(Security classification of title, body of abstract and indexing annotation must be entered when the overall report is classified)

1. ORIGINATING ACTIVITY (Corporate author) U. S. Army Materials Research Agency Watertown, Massachusetts 02172	2a. REPORT SECURITY CLASSIFICATION Unclassified 2b. GROUP

3. REPORT TITLE

STRESS CONCENTRATION FACTORS IN T-HEADS

4. DESCRIPTIVE NOTES (Type of report and inclusive dates)

5. AUTHOR(S) (Last name, first name, initial)

Baratta, Francis I.

6. REPORT DATE	7a. TOTAL NO. OF PAGES	7b. NO. OF REFS
November 1966	16	11

8a. CONTRACT OR GRANT NO. b. PROJECT NO. D/A 1N542718D387 c. AMCMS Code 5547.12.62700 d. Subtask 35425	9a. ORIGINATOR'S REPORT NUMBER(S) AMRA TR 66-36 9b. OTHER REPORT NO(S) (Any other numbers that may be assigned this report)

10. AVAILABILITY/LIMITATION NOTICES

Distribution of this document is unlimited.

11. SUPPLEMENTARY NOTES	12. SPONSORING MILITARY ACTIVITY
	Picatinny Arsenal Dover, New Jersey 07801

13. ABSTRACT Two simple formulae are presented which predict stress concentration factors applicable to a two-dimensional symmetrical T-head configuration. This configuration consists of a deep head joined to a shank by fillet radii. The independent equations that predict stress concentration factors for the same geometry are derived for two different loading conditions. In one instance, a tensile force is applied to the shank end of the T-shape. Equilibrium of forces is attained by supporting the bottom edge of the head section, resulting in the shank section being pulled in tension. In the second instance, a compressive load is applied to the top edge of the head section while the configuration is again supported at the bottom edge. Thus, only the head section is stressed and in a compressive manner.

Because the analysis is not exact, the magnitudes of the stress concentration factors resulting from the predictive equations appear to be overly conservative at some ranges of the geometry parameter ratios. Therefore, an arbitrary "limit of application", as it is termed in the text, is recommended when using these equations.

Again, because of the inexactness of the analysis, experimental stress concentration factors are indirectly obtained for the first loading condition and directly obtained for the second loading condition mentioned above. These data were obtained for several geometric ratios of the T-head configuration and compared to the corresponding predicted values.

It was found that the formulae could be utilized, with engineering accuracy, within a certain range of the two pertinent geometry ratios. Beyond these ranges, the error becomes excessive, but conservative. (Authors)

DD FORM 1 JAN 64 1473

UNCLASSIFIED
Security Classification

UNCLASSIFIED
Security Classification

14. KEY WORDS	LINK A		LINK B		LINK C	
	ROLE	WT	ROLE	WT	ROLE	WT
Experimental mechanics Stresses Stress concentrations Stress intensity Experimental stress analysis Photoelasticity						

INSTRUCTIONS

1. ORIGINATING ACTIVITY: Enter the name and address of the contractor, subcontractor, grantee, Department of Defense activity or other organization *(corporate author)* issuing the report.

2*a*. REPORT SECURITY CLASSIFICATION: Enter the overall security classification of the report. Indicate whether "Restricted Data" is included. Marking is to be in accordance with appropriate security regulations.

2*b*. GROUP: Automatic downgrading is specified in DoD Directive 5200.10 and Armed Forces Industrial Manual. Enter the group number. Also, when applicable, show that optional markings have been used for Group 3 and Group 4 as authorized.

3. REPORT TITLE: Enter the complete report title in all capital letters. Titles in all cases should be unclassified. If a meaningful title cannot be selected without classification, show title classification in all capitals in parenthesis immediately following the title.

4. DESCRIPTIVE NOTES: If appropriate, enter the type of report, e.g., interim, progress, summary, annual, or final. Give the inclusive dates when a specific reporting period is covered.

5. AUTHOR(S): Enter the name(s) of author(s) as shown on or in the report. Enter last name, first name, middle initial. If military, show rank and branch of service. The name of the principal author is an absolute minimum requirement.

6. REPORT DATE: Enter the date of the report as day, month, year; or month, year. If more than one date appears on the report, use date of publication.

7*a*. TOTAL NUMBER OF PAGES: The total page count should follow normal pagination procedures, i.e., enter the number of pages containing information.

7*b*. NUMBER OF REFERENCES: Enter the total number of references cited in the report.

8*a*. CONTRACT OR GRANT NUMBER: If appropriate, enter the applicable number of the contract or grant under which the report was written.

8*b*, 8*c*, & 8*d*. PROJECT NUMBER: Enter the appropriate military department identification, such as project number, subproject number, system numbers, task number, etc.

9*a*. ORIGINATOR'S REPORT NUMBER(S): Enter the official report number by which the document will be identified and controlled by the originating activity. This number must be unique to this report.

9*b*. OTHER REPORT NUMBER(S): If the report has been assigned any other report numbers *(either by the originator or by the sponsor)*, also enter this number(s).

10. AVAILABILITY/LIMITATION NOTICES: Enter any limitations on further dissemination of the report, other than those imposed by security classification, using standard statements such as:

(1) "Qualified requesters may obtain copies of this report from DDC."

(2) "Foreign announcement and dissemination of this report by DDC is not authorized."

(3) "U. S. Government agencies may obtain copies of this report directly from DDC. Other qualified DDC users shall request through ________________."

(4) "U. S. military agencies may obtain copies of this report directly from DDC. Other qualified users shall request through ________________."

(5) "All distribution of this report is controlled. Qualified DDC users shall request through ________________."

If the report has been furnished to the Office of Technical Services, Department of Commerce, for sale to the public, indicate this fact and enter the price, if known.

11. SUPPLEMENTARY NOTES: Use for additional explanatory notes.

12. SPONSORING MILITARY ACTIVITY: Enter the name of the departmental project office or laboratory sponsoring *(paying for)* the research and development. Include address.

13. ABSTRACT: Enter an abstract giving a brief and factual summary of the document indicative of the report, even though it may also appear elsewhere in the body of the technical report. If additional space is required, a continuation sheet shall be attached.

It is highly desirable that the abstract of classified reports be unclassified. Each paragraph of the abstract shall end with an indication of the military security classification of the information in the paragraph, represented as *(TS)*, *(S)*, *(C)*, or *(U)*.

There is no limitation on the length of the abstract. However, the suggested length is from 150 to 225 words.

14. KEY WORDS: Key words are technically meaningful terms or short phrases that characterize a report and may be used as index entries for cataloging the report. Key words must be selected so that no security classification is required. Identifiers, such as equipment model designation, trade name, military project code name, geographic location, may be used as key words but will be followed by an indication of technical context. The assignment of links, rules, and weights is optional.

UNCLASSIFIED
Security Classification